Vector-Meson Production in a Model of Higher Baryon Couplings

Krishna Sen Gupta
Department of Physics and Astrophysics, University of Delhi, Delhi-7, India

and

V. K. Gupta
Centre for Advanced Study in Physics, University of Delhi, Delhi-7, India
(Received 23 October 1970)

The phenomenological model for the couplings of hadron resonances (B_L) to the 56 baryons (B) and 36 mesons [pseudoscalar (P) or vector(V)], proposed by Mitra, is used for the investigation of certain $\pi + N \to V + N'$ reactions in the intermediate-energy region via the s channel, with the inclusion of baryon resonances with orbital angular momentum $L = 0, 1, 2$. The specific reactions considered are $\pi^+ p \to \rho^+ p$, $\pi^- p \to \rho^0 n$, and $\pi^+ n \to \omega p$. The results for differential cross sections and density matrices as functions of $\cos\theta$ are presented for each of the above reactions over a wide range of incident pion momentum (2.75–8 GeV/c). The structure of the PBB_L and VBB_L couplings for $L^P \to 0^+$ transition are characterized by a Lorentz-invariant form factor f_L, for which two different forms, also postulated by Mitra, are considered. For a comparison of the two form factors the $\pi^+ p \to \rho^+ p$ results are presented for both of them at all energies considered. The more recent (new) form factor gives a definitely better fit to the data than the earlier (old) one. A striking observation in this regard is that the old form factor predicts the wrong sign for $\mathrm{Re}\rho_{10}$, viz., positive in all cases, whereas the new form factor not only reverses the sign of $\mathrm{Re}\rho_{10}$ to bring it in agreement with experiment, but produces good agreement even in absolute value. As $\mathrm{Re}\rho_{10}$ is expected to depend much more crucially than other quantities on the relative phases and magnitudes of various partial amplitudes, the superiority of the new form factor over the old one is indicated. For the energy dependence, the agreement with experiment becomes consistently poorer at higher energies until at about 8-GeV/c lab momentum the two differ by an order of magnitude. This can perhaps be attributed to the neglect of higher resonances in the present calculation. The present calculation, which is done in the s channel, agrees well with other calculations performed in the t channel in the near forward direction as well as with the u-channel calculation in the near backward direction, thus providing a good case for duality. The conclusions drawn from the density-matrix analysis are qualitatively similar to those from the analysis of the differential cross section.

I. INTRODUCTION

In the preceding paper[1] the relativistic hadron coupling scheme of Mitra[2-4] has been applied to pion photoproduction. In the present paper we apply the same model to the production of vector mesons in meson-nucleon collisions. The essential ingredients of the model, as discussed in the previous article, are (1) use of a supermultiplet representation based on SU(6)×O(3) for the hadron spectrum with baryons given by the representations (56, $2L^+$) and (70, $(2L+1)^-$) together with their radial excitations, (2) a relativistic extension of the SU(6)×O(3) model for the $BB_L P$ interaction, characterized by the appearance of a relativistically invariant form factor f_L for a given $L^P \to 0^+$ transition, (3) use of Schwinger's idea of partial symmetry to obtain the corresponding $BB_L V$ coupling in a consistent manner, and (4) determination of the relativistic form factor f_L.

In the absence of any underlying dynamical theory, the form factor can be fixed only in a phenomenological manner, though several restrictions can be placed on its possible structure from certain theoretical considerations. The form factor which was earlier postulated by Mitra[2,3] has been applied extensively to baryon and meson phenomena,[5-7] especially to the calculation of total and partial decay widths, with quite encouraging results.

Because of its success in the study of resonance decay widths, we feel it should be interesting to apply this model to some other processes where it can be tested for its effects off the mass shell. One such class of processes, which we have chosen to analyze here, is vector-meson production in meson-baryon collisions, e.g.,

$$\pi N \to \rho N ,$$

$$\pi N \to \omega N .$$

A reasonable amount of data is available on these processes and many other calculations have also been performed so that a meaningful comparison can be made.

The main experimental feature of these reactions in the intermediate-energy region is their peripheral nature. This is best shown by a strong peak in the forward direction in the differential cross section for all these reactions. Because of this the one-particle-exchange models (OPE) have been rather successful in explaining the gross features of these processes.[8] But whereas the OPE was partially successful in explaining the peak in the differential cross section, the decrease of production cross sections with increasing momentum transfer is much more rapid than expected on the basis of OPE, especially when the exchanged particle is required to be a vector meson.[9] This drawback was partially met in the OPE by the inclusion of other competing open channels (OPE with absorption).[9-12] This gave a marked qualitative improvement (at the cost of extra parameters) but a significant quantitative disagreement, especially in the forward direction, persisted.

A number of calculations[13-15] have also been performed in the Regge-pole-exchange model with various degrees of complexity. The model has some of the features of OPE built in, and hence it is not surprising that it reproduced similar results.[13]

For obvious reasons most of these peripheral and Regge-pole calculations have been performed in the t channel. In our model on the other hand we approximate the $PB \to VB$ amplitude by a sum of contributions from various s-channel resonances which couple to the initial and final systems. In the present calculation we consider all baryon resonances with orbital angular momentum up to and including $L=2$, which are the only ones known with confidence as to their masses and other quantum numbers. This restricts the validity of the model to the intermediate-energy region (say, up to a laboratory momentum of a few GeV/c), the same region in which t-channel exchanges dominate the processes. In our model, which is an s-channel calculation, the t exchanges (and u exchanges) can be hopefully simulated by the combined effect of all the resonances via duality.[16,17] Hence, from this point of view, the present calculation may also be considered to provide a good experimental test of the idea of duality.

An important feature of the relativistic coupling scheme[2,4] used in the present analysis is the almost total lack of adjustable parameters. The only unknowns in the model are the over-all coupling constants g_L which are fixed once for all by fitting the decay widths of some well-known resonances (only one constant for each L value).[2,3] The amplitude for any process is then completely specified even with regard to its phase. The total $PB \to VB$ amplitude which is a sum of contributions from individual resonant amplitudes is thus extremely sensitive to the phase of these individual amplitudes. As a result, the differential cross sections and the density matrices depend very delicately on both the magnitude and the phase of the amplitudes. This is in contrast to the case of decay widths, for which no such delicate balance is required, and which are therefore not as sensitive to the detailed structure of the form factor as vector-meson production is.

Apart from this, in the present calculation (as also in the photoproduction processes) the baryon resonances in the intermediate state are off the mass shell, and so the form factors which appear in the PBB_L and VBB_L couplings will also be off the mass shell. Again this is in contrast to the situation for decay widths, where only the on-mass-shell value of the form factor is required. Because of these reasons the analysis of vector-meson production processes provides a more stringent test of the model, in particular of the structure of the form factor, than is possible from the study of decay widths alone.

Though the form factor proposed earlier by Mitra[3] and applied extensively to various processes had a striking degree of experimental success, it was not very satisfactory on some theoretical grounds as discussed in the preceding paper. Recently Mitra has proposed an alternative expression for the form factor which not only meets the theoretical objections to the "old" one, but also gives a significant improvement in some of the crucial decay-width ratios.[18] Since the off-mass-shell forms of the "new" and the "old" form factors are radically different, we have, as a test case, carried out one of the calculations (viz., $\pi^+ p \to \rho^+ p$) with both the old and the new form factors, in order to test the sensitivity of the results to them.

In Sec. II we briefly outline the derivation of the invariant amplitudes for the $PB \to VB$ processes starting from the basic quark-hadron couplings. In Sec. III the results both for the differential cross section and the density-matrix elements at various energies are presented. The processes studied are $\pi^\pm p \to \rho^\pm p$, $\pi^- p \to \rho^0 n$, and $\pi^+ n \to \omega p$. Wherever possible, a comparison with experiment, as well as with the results of various other models, is made. The conclusions regarding the model, with particular reference to the form factors, are discussed.

II. FORMALISM

In this section we first briefly review the derivation of the PBB_L and VBB_L couplings for the sake of completeness. Using these couplings the

$PB \to VB$ amplitudes are written in terms of the invariant amplitudes given by Liu and Singer.[19] The differential cross sections and density matrices are then expressed in terms of these amplitudes making use of the helicity formalism.

The M matrix of Schwinger for BBP and BBV vertices may be written in momentum space [except for an over-all factor of (-1)] as

$$M = ik_i\pi^a\sigma_i\tau_a + i\epsilon_{ijk}k_i\sigma_j(\rho_k^a\tau_a + \omega_k 1) + m_\rho\rho_0^a\tau_a + m_\omega\omega_0 1, \tag{2.1}$$

where the notation used is the same as in the preceding paper (except that we write k in place of q). For pion couplings the spin-matrix elements arising from the direct term for $B_L \to B\pi$ transitions must be expressible in one of the following forms:

$$\chi^\dagger\vec{\sigma}\cdot\vec{k}\chi, \quad \chi^\dagger k_i\chi_i, \tag{2.2}$$

where χ and χ_i are the (nonrelativistic) Pauli and Rarita-Schwinger spinors, respectively. The complete coupling for PBB_L can be evaluated by multiplying (2.2) with the spatial part of the matrix element which has the structure

$$f_L(k^2)B^{LM}_{i_1\cdots i_L}k_{i_1}\cdots k_{i_L}, \tag{2.3}$$

where $f_L(k^2)$ is a (scalar) form factor in $\vec{k}^2$ and $B^{LM}_{i_1\cdots i_L}$ a tensor of rank L.

The calculation of the couplings then merely reduces to a Clebsch-Gordan reduction of the direct products like $\chi_i\otimes B^L_{(i)}$ and $\chi\otimes B^L_{(i)}$, whose relativistic extension, carried out in detail in Ref. 2, will finally give the following structure for the PBB_L couplings:

$$[B^L_{\alpha_1\cdots\alpha_L}\otimes\chi]^\dagger(\vec{\sigma}\cdot\vec{k})(k_{\alpha_1}\cdots k_{\alpha_L})\chi \Rightarrow \bar{\psi}^{L+1/2}_{\mu_1\cdots\mu_L}(-i\gamma_s\gamma\cdot k)k_{\mu_1}\cdots k_{\mu_L}\psi + (-m_\pi^2)\left(\frac{L}{2L+1}\right)^{1/2}\bar{\psi}^{L-1/2}_{\mu_2\cdots\mu_L}k_{\mu_2}\cdots k_{\mu_L}\psi,$$

$$[B^L_{\alpha_1\cdots\alpha_L}\otimes\chi_\alpha]^\dagger k_\alpha k_{\alpha_1}\cdots k_{\alpha_L}\chi \Rightarrow \bar{\psi}^{L+3/2}_{\mu\mu_1\cdots\mu_L}k_\mu k_{\mu_1}\cdots k_{\mu_L}\psi + \left(\frac{L+1}{2L+3}\right)^{1/2}\bar{\psi}^{L+1/2}_{\mu_1\cdots\mu_L}(-i\gamma_s k\cdot\gamma)k_{\mu_1}\cdots k_{\mu_L}\psi \tag{2.4}$$

$$+(-m_\pi^2)\left(\frac{L(L+1)}{2(2L+1)}\right)^{1/2}\bar{\psi}^{L-1/2}_{\mu_2\cdots\mu_L}k_{\mu_2}\cdots k_{\mu_L}\psi + (-m_\pi^2)\left(\frac{L(L^2-1)}{2(4L^2-1)}\right)^{1/2}\bar{\psi}^{L-3/2}_{\mu_3\cdots\mu_L}(-i\gamma_s\gamma\cdot k)k_{\mu_3}\cdots k_{\mu_L}\psi. \tag{2.5}$$

These couplings must be considered in conjunction with the necessary SU(6) factors and isotopic structures for various cases which are listed in Ref. 6.

In the case of vector mesons there are two types of couplings: (i) "magnetic coupling" provided by the three-vector $\vec{k}'\times\rho^a$ and (ii) "minimal coupling" symbolized by the three-scalar $m_\rho\rho_0^a$.[4] The spatial part of the matrix element is still given by the form (2.3), while the spin structures are now given by one of the forms (the four-momentum of the vector meson is now denoted by k')

$$\chi^\dagger\chi, \quad \chi^\dagger\vec{\sigma}\cdot\vec{k}'\times\vec{\epsilon}\chi, \quad \chi^\dagger e_{ijk}k'_i\epsilon_j\chi_k, \tag{2.6}$$

where ϵ represents the polarization vector for the vector meson. The product of (2.6) with (2.3) and its relativistic extension will give the following expressions for the VBB_L couplings:

$(\underline{56}, L^+) \to (\underline{56}, 0^+)$.

(a) $\underline{8} \to \underline{8}$: $(l_1A + l_2B) + \left(\frac{L}{2L+1}\right)^{1/2}(l_1C + l_3C')$, (2.7)

(b) $\underline{10} \to \underline{8}$: $2\sqrt{2}\left[D + \left(\frac{L+1}{2L+3}\right)^{1/2}A\right]$. (2.8)

$(\underline{70}, 1^- \to \underline{56}, 0^+)$.

(a) $\underline{8}_d \to \underline{8}$: $(l_4A + l_5B) + \left(\frac{L}{2L+1}\right)^{1/2}(l_4C + l_6C')$, (2.9)

(b) $\underline{8}_d \to \underline{8}$: $l_7\left[D + \left(\frac{L+1}{2L+3}\right)^{1/2}A\right]$, (2.10)

(c) $\underline{10} \to \underline{8}$: $\sqrt{3}\ (\frac{1}{3}A + B) - \left(\frac{L}{2L+1}\right)^{1/2}\left(\frac{1}{\sqrt{3}}C + \frac{2}{\sqrt{3}}C'\right)$, (2.11)

where A, B, C, and D are the different types of $\bar{B}BB_LV$ couplings defined by Eq. (2.5) of the preceding paper. For convenience the C type of coupling is redefined in two parts as follows:

$$C = i\bar{\psi}\gamma_5 k'^{\prime}\gamma_\mu\epsilon_\mu k'_{\mu_2}\cdots k'_{\mu_L}\psi^{L-1/2}_{\mu_2\cdots\mu_L},$$

$$C' = \bar{\psi}\gamma_5 m_V\gamma\cdot k'\gamma\cdot\epsilon\, k'_{\mu_2}\cdots k'_{\mu_L}\psi^{L-1/2}_{\mu_2\cdots\mu_L},$$

where m_V denotes the vector-meson mass. The production of ω in the s channel occurs only through the octet ($I = \frac{1}{2}$) intermediate states. Therefore the VBB_L couplings ($\underline{10} \to \underline{8}$) given by Eqs. (2.8) and (2.11) are exclusively meant for ρ production. The $\underline{8} \to \underline{8}$ couplings, i.e., Eqs. (2.7), (2.9), and (2.10) [for ρ and ω productions] are to be considered in conjunction with the necessary SU(6) factors ($l_1\cdots l_7$) for the magnetic and minimal couplings (listed in Table I) as well as with the isotopic-spin structures for the various cases.

The amplitude for the process $\pi + N \to V + N'$ can

be evaluated from the VBB_L and PBB_L vertices (V_I and V_{II}, respectively) as follows: The reduced matrix elements F_J for each resonance can be expressed as

$$F_J = V_I \Theta^J(Q) \frac{2M_J}{M_J^2+Q^2} V_{II}, \tag{2.12}$$

where $[2M_J/(M_J^2+Q^2)]\Theta^J(Q)$ is the propagator for an s-channel resonance[20] B_L of spin $J=L+\frac{1}{2}$, mass[21] M_J, and four-momentum Q which can be most conveniently obtained in terms of the well-known projection operator for a particle of integral spin[22,23] L in the form

$$\Theta^J(Q) = \frac{L+1}{2L+3}\gamma^\nu\gamma_\mu\Theta^{\mu\mu_1\cdots\mu_L}_{\nu\nu_1\cdots\nu_L}(L+1)\frac{i\gamma\cdot Q - M}{2M_J}. \tag{2.13}$$

For each s-channel resonance B_L^J considered in the intermediate state, we pick up the relevant PBB_L and VBB_L couplings given earlier [Eqs. (2.4)–(2.11)]. Next the projection operator $\Theta^{\mu_1\mu_2\cdots\mu_L}_{\nu_1\nu_2\cdots\nu_L}(L+1)$ is written in terms of Legendre polynomials $P_L(\bar{z})$.[23] Further simplifications can be achieved by making replacements such as

$$\gamma_\mu(k_{\mu_1}\cdots k_{\mu_L}) \to \frac{1}{L+1}\left(\gamma\cdot\frac{\partial}{\partial k_\mu}\right)(k_\mu k_{\mu_1}\cdots k_{\mu_L})$$

given in detail in the preceding paper. With the help of some well-known properties of the γ matrices, and making frequent use of the Dirac equation, one finally arrives at the following expressions for the ρ and ω production amplitudes for the various intermediate states considered:

$$\begin{aligned}
&N(938): \tfrac{1}{3}(4+Q^2/M^2)[(a_1+Ma_2)V_1 \\
&\qquad + m_V(a_3-Ma_4)V_2], \\
&S_{11}^d(1715): \tfrac{1}{3}(4+Q^2/M^2)[-m_V(b_1+MA_1)V_3 \\
&\qquad + (b_3+MA_3)V_4]m_\pi^2 m_V, \\
&D_{13}^d(1515): V_4 I_1 + V_5 m_V I_2, \\
&D_{13}^q(1675): \tfrac{3}{20}V_4 I_1, \\
&D_{15}^q(1675): \frac{V_6}{315}(-I_1'+2I_2'-I_3), \\
&F_{13}(1855): -\tfrac{1}{2}m_\pi^2 m_V(m_V V_3 I_3 + V_4 I_4), \\
&F_{15}(1690): (V_2 m_V I_5 + I_6 V_1).
\end{aligned} \tag{2.14}$$

The coefficients $V_1\cdots V_6$ are listed in Table II for ρ and ω productions. The amplitudes for vector-meson production via decuplet intermediate states (given below) are exclusively for ρ production.

$$\begin{aligned}
&S_{31}(1630): \tfrac{1}{27}(4+Q^2/M^2)[2(b_3+MA_3) \\
&\qquad - m_\rho(b_1+MA_1)]m_\pi^2 m_\rho, \\
&D_{33}(1670): \tfrac{1}{9}I_1 + \tfrac{1}{3}m_\rho I_2, \\
&F_{35}(1880): -\tfrac{24}{7}I_6, \\
&F_{37}(1940): \frac{2}{315}(-I_7+I_8-I_9), \\
&P_{33}(1238): -\frac{8}{15}\left[2\left(1-\frac{S}{M^2}\right)I_9 - I_{10} + I_{11}\right].
\end{aligned} \tag{2.15}$$

All the above amplitudes are to be multiplied by the appropriate form factors for PBB_L and VBB_L vertices (discussed later) as well as the factor $1/(Q^2+M_J^2)$. The amplitude for $P_{11}(1470)$ is the same as that for $N(938)$ except that the coupling constant g_R is different from g_0. The quantities a_i, b_i, c_i, and I_i are certain combinations of the invariant amplitudes (A_i) introduced by Singer, and are given in Appendix A. F_i are certain functions of the kinematic variables which are also given in Appendix A.

For the processes under investigation, namely, $\pi+N \to V+N'$, it is most convenient to consider the helicity amplitudes defined as

$$\langle \lambda, \lambda_f | \lambda_i \rangle = \langle \lambda, \lambda_f | T | \lambda_i, 0 \rangle = \bar{u}(p_2) T u(p_1),$$

where λ, λ_f, and λ_i represent the helicities of the vector meson and the final and incident nucleons, respectively; $T=\sum O_i X_i$, $u(p_1)$ and $u(p_2)$ are the helicity Dirac spinors for the initial and final nu-

TABLE I. The SU(6) factors $(l_1,\ldots,l_7)$ for VBB_L couplings for ρ and ω production processes.

l_i	ρ	ω
l_1	$5/\sqrt{3}$	-1
l_2	$-\sqrt{3}$	3
l_3	$-8/\sqrt{3}$	4
l_4	$2\sqrt{2}/\sqrt{3}$	$-\sqrt{2}$
l_5	$-\sqrt{6}$	0
l_6	$-5\sqrt{2}/\sqrt{3}$	$\sqrt{2}$
l_7	-1	$-\sqrt{3}$

TABLE II. The constants V_i of the $PB \to VB$ amplitudes via octet resonance defined in Eq. (2.14).

V_i	ρ	ω
V_1	$-\frac{25}{3}$	$-5/\sqrt{3}$
V_2	5	$5\sqrt{3}$
V_3	$-\frac{8}{9}$	$-4/3\sqrt{3}$
V_4	$-\frac{20}{9}$	$-4/3\sqrt{3}$
V_5	$\frac{4}{3}$	0
V_6	$\frac{3}{8}$	$3\sqrt{3}/8$

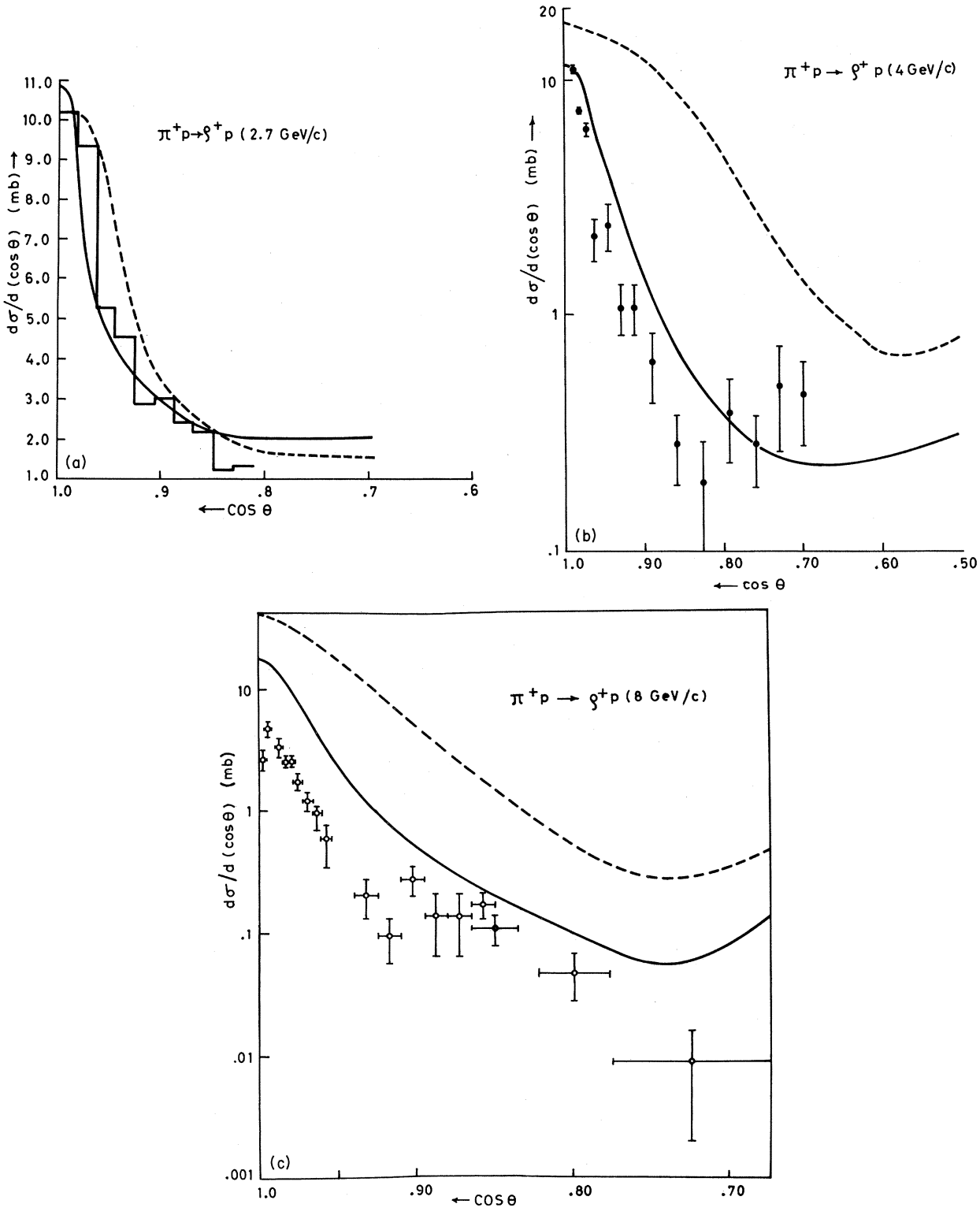

FIG. 1. (a) The differential cross section $d\sigma/d\cos\theta$ in mb for the process $\pi^+p \to \rho^+p$ at incident pion momentum 2.75 GeV/c. The experimental histogram is from the compilation in Ref. 11. In this figure and in (b) and (c) the dashed and solid curves represent the results for "old" and "new" form factor, respectively. (b) Same as (a) at 4.0 GeV/c. The experimental points are from the compilation in Ref. 13. (c) Same as (a) at 8.0 GeV/c. The experimental points are from Ref. 32.

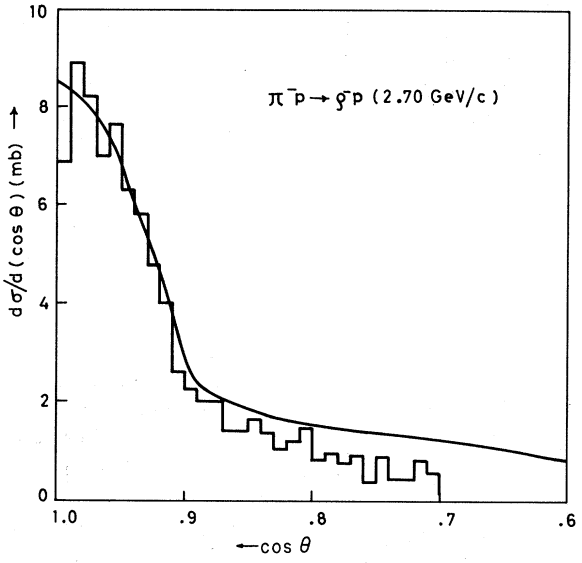

FIG. 2. The differential cross section $d\sigma/d\cos\theta$ in mb for the process $\pi^- p \to \rho^- p$ at incident pion momentum 2.70 GeV/c. The experimental histogram is from Refs. 13 and 31. In this figure and in Figs. 3 and 4, the curves represent results with "old" form factor.

cleons, while p_1 and p_2 are their four-momenta, respectively. $\bar{u}(p_2)O_i u(p_1)$ are the invariant amplitudes and X_i their coefficients.

The differential cross section and the decay density matrix of the vector meson in the c.m. frame are given, respectively, by

$$\frac{d\sigma}{d\Omega} = \frac{m^2}{16\pi^2 s} \frac{|\vec{k}'|}{|\vec{k}|} \sum |\langle \lambda, \lambda_f | \lambda_i \rangle|^2 ,$$

$$\rho_{\lambda\lambda'} = \frac{1}{N} \sum \langle \lambda, \lambda_f | \lambda_i \rangle \langle \lambda', \lambda_f | \lambda_i \rangle^* ,$$

where s is the square of the total c.m. energy and N is a normalization constant, determined by the condition $\mathrm{Tr}(\rho) = 1$.

The values of $\bar{u}(p_2)O_i u(p_1)$ for different helicity states are listed in Appendix B. These, in conjunction with the amplitudes given earlier [Eqs. (2.14) and (2.15)], will give us the desired helicity amplitudes.

The only quantities yet to be specified for a numerical evaluation are the form factors $f_L(k^2)$ for PBB_L and VBB_L couplings. As mentioned before we have two types of form factors at our disposal. The expressions for the old and the new form factors for both PBB_L and VBB_L vertices are given in the preceding paper.

III. RESULTS AND DISCUSSION

We have applied the model to the study of the following processes:

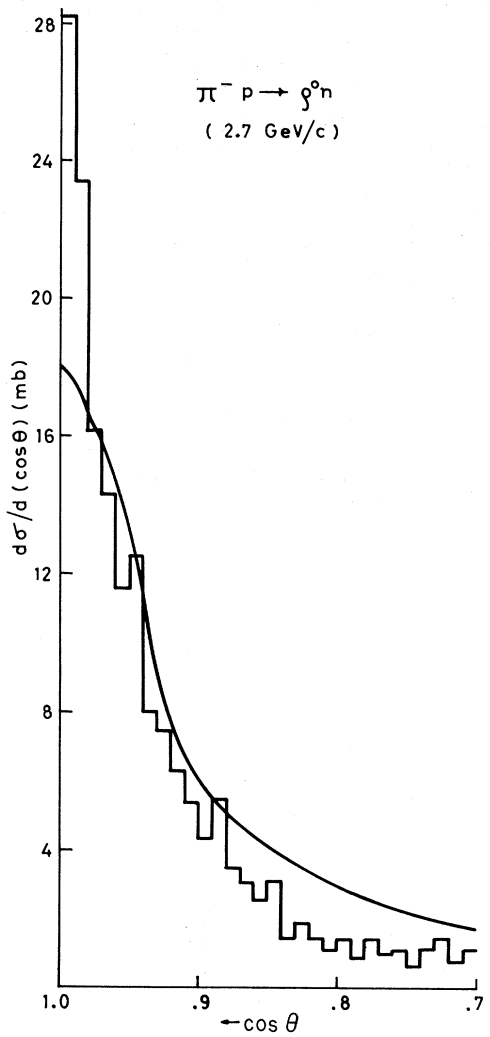

FIG. 3. Same as Fig. 2 for the process $\pi^- p \to \rho^0 n$.

$\pi^+ p \to \rho^+ p$,

$\pi^- p \to \rho^- p$,

$\pi^- p \to \rho^0 n$,

$\pi^+ n \to \omega p$.

For each process we have calculated the differential cross section and density-matrix elements as functions of $\cos\theta$ (center of mass) at different energies.

As pointed out earlier, the main experimental feature of these reactions in the intermediate-energy region is their rather overperipheral nature, as indicated by a strong peak in the forward direction observed in the differential cross section. Because of this circumstance, most of the earlier calculations on vector-meson production have been in the t channel. Thus one has the one-particle-exchange (OPE) model[8,9] and its improved version

through the inclusion of other competing channels (OPE with absorption),[10-12] the Regge-pole model with the inclusion of various trajectories, Regge cuts, and so on.[13,15] A u-channel calculation of these processes in the Regge-pole model has also been performed.[24] But even with the inclusion of various corrections, the t- and u-channel calculations have had their validity limited only to a small range of angles in the near forward and near backward directions, respectively.

In our model, on the other hand, we do not include any t-channel effects but only low-lying s-channel resonances. If the idea of duality is even qualitatively correct this should be able to simulate the effect of the t- and u-channel exchanges. Thus the results of the present calculation should be valid over a wider range of angles, especially in the near forward and backward directions.

Another feature of the present model is the absence of any adjustable parameters. The only parameters that appear in the theory are the coupling constants (for even and odd couplings) which are adjusted from the decay rates of some well-known baryon and meson resonances. This enhances the predictive nature of the model. This feature is to be contrasted with those of other models, especially the "dynamical quark models,"[25-28] in which a large number of parameters appear and it is, in general, not possible to predict any specific numbers, but only certain sum rules, most of which follow from symmetry arguments alone.

Of course, as emphasized earlier, there are *ad hoc* form factors which appear in our model, and at the present state of knowledge it is not possible to fix them theoretically. Still, if one requires the form factors to incorporate some of the well-known theoretical and experimental features of hadrons, the choice is considerably narrowed down. We have at the moment the "old" form factor given by Mitra[2,3] some time ago and the "new" form factor proposed more recently.[18] Our present calculation can help in deciding in favor of one or the other, as the results are expected to be sensitive to the choice of the form factor. Keeping this in mind we have performed a model calculation for $\pi^+ p \to \rho^+ p$ with the "new" form factor as well.

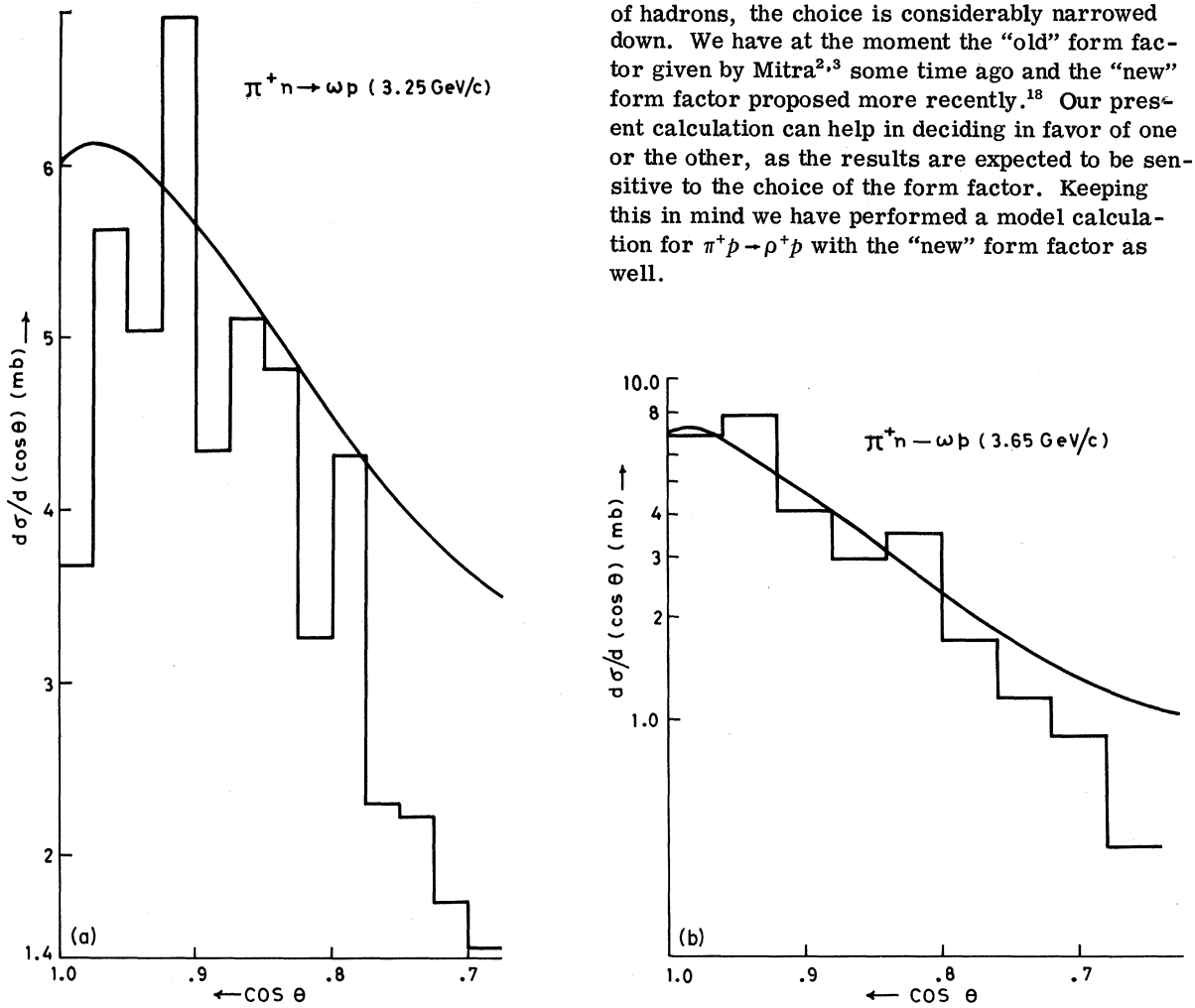

FIG. 4. (a) The differential cross section $d\sigma/d\cos\theta$ in mb for the process $\pi^+ n \to \omega p$ at incident pion momentum 3.25 GeV/c. The experimental histogram (Ref. 11) is in arbitrary units. (b) Same as in (a) at 3.65 GeV/c. The experimental histogram is from Ref. 15 and is in arbitrary units.

Differential Cross Sections

The results of our model for the differential cross section for various processes at different energies as a function of $\cos\theta$ are shown in Figs. 1–5 along with the experimental values wherever available. First of all we find that at low energies the predictions of our model are in very good agreement with the data for almost the entire range of angles ($1 \geq \cos\theta \geq 0.7$) plotted. For the processes $\pi^+ p \to \rho^+ p$ at 2.75 GeV/c (Ref. 11) and $\pi^- p \to \rho^- p$ at 2.7 GeV/c (Refs. 29 and 13) in the forward direction ($\theta = 0$), the prediction of our model is within experimental errors of the observed values, in contrast to the peripheral model where the deviation is as much as 40%.[11] For the charge-exchange process $\pi^- p \to \rho^0 n$, on the other hand, our model predicts too small a value for the differential cross section in the forward direction. An interesting observation in this regard is that though we have added a fairly large number of resonances in the s channel, our numerical values indicate that

$$\frac{d\sigma}{d(\cos\theta)}(\pi^- p \to \rho^0 n) \approx 2\frac{d\sigma}{d(\cos\theta)}(\pi^- p \to \rho^- p),$$

a relation which, in the peripheral model, is an exact one because only the pion exchange contributes to it.[11] This near-numerical equality of the s- and t-channel results is strongly suggestive of duality. Experimentally this relation seems to be quite well satisfied except in the near-forward direction.

With increasing energy we find that our fit to the data becomes consistently poorer until at about 8-GeV/c lab momenta the experimental numbers[30] and theoretical predictions differ by an order of magnitude. This is not very surprising, despite our relativistic kinematics, as we have included only low-mass resonances (up to and including $L = 2$). Because of this constraint, we cannot expect our present calculation to be reliable enough at such high energies. As is well known, the peripheral model (with absorption) is also expected to work only in this region. In our model at least there is a scope for increasing its range of validity by taking more resonances into account without adding any new parameters. But in actual practice this becomes a difficult task unless some algebraic method can be found for adding the effects of all the resonances. Such a possibility exists with the new form factor as has been demon-

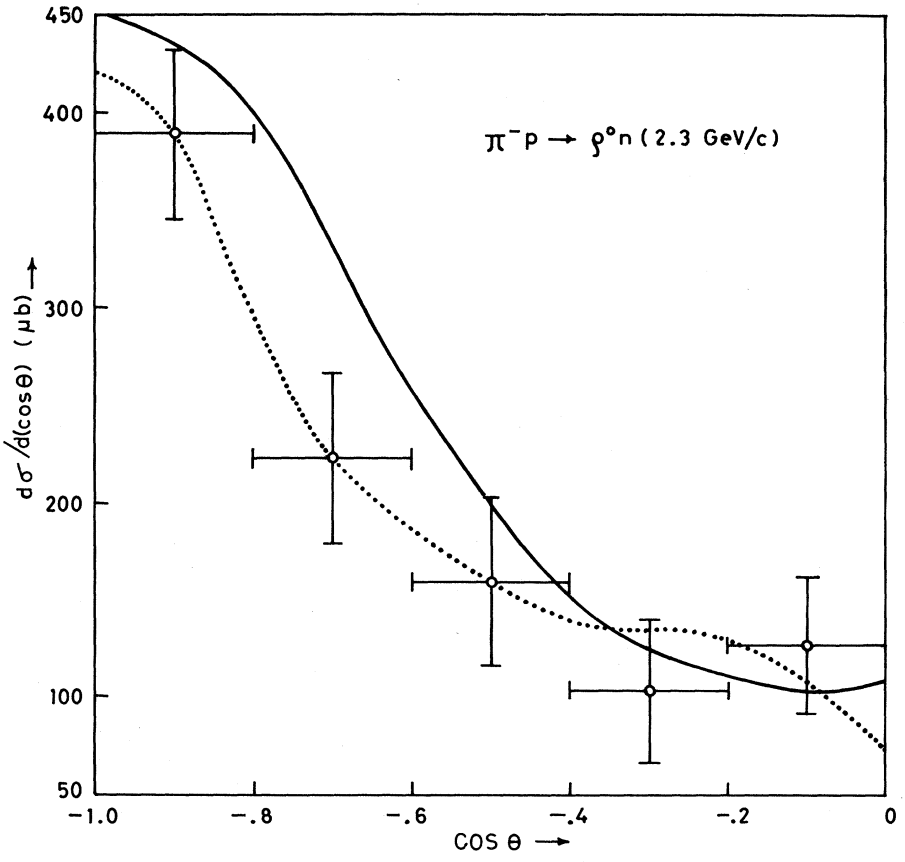

FIG. 5. The backward differential cross section $d\sigma/d\cos\theta$ in μb for the process $\pi^- p \to \rho^0 n$ at 2.3 GeV/c. The experimental points are from Ref. 24. The solid curve is our result with the new form factor, and the dotted curve is that of Kelly *et al.* (see Ref. 24).

strated in a model u-channel calculation.[18]

For a comparison of the "new" and "old" form factors we have presented the results for $\pi^+p \to \rho^+p$ with both of them at all energies. We find that the "new" form factor marks a significant improvement in the comparison with the experimental data in all cases. At 2.75 GeV/c, where the "old" form factor also predicted very good results, there is a significant quantitative improvement with the "new" form factor which makes the fit almost perfect. At 4.0 GeV/c the "old" form factor gives results higher than the experimental figures[13] by as much as a factor of 3, but the "new" form factor brings them down almost to the experimental level. At 8.0 GeV/c, despite a vast improvement in the results with the "new" form factor, the discrepancy between the theory and experiment remains uncomfortably large, presumably because of the insufficient number of resonances included. Thus we find that the sensitivity of the results to the choice of the form factor increases with increasing energy; at low energies the results are rather insensitive to this choice, in conformity with the conclusion of Mehrotra and Mitra for the photoproduction process.[1]

For the $\pi^+n \to \omega p$ case, which is also a charge-exchange reaction, the differential cross sections are unfortunately available only in arbitrary units,[11,14,15] so that a quantitative comparison can not be made. However, at 3.25 GeV/c (Ref. 11) [Fig. 4(a)] there is a sharp peak in the differential cross section in the near-forward direction, which is also present in our analysis though it is not as pronounced. But for this slight discrepancy, the general shapes of the experimental and theoretical curves agree quite well. At 3.65 GeV/c (Ref. 15) [Fig. 4(b)] where also the results are available only in arbitrary units, the peak already seems to vanish and hence the agreement of our model with the experiment is much better.

We have also calculated the $\pi^-p \to \rho^0n$ differential cross section at 2.3 GeV/c against $\cos\theta$ in the near-backward direction (with the new form factor); it is shown in Fig. 5 along with the experimental points.[24] The results of an earlier u-channel calculation for this process, using the "strong-cut Reggeized absorption model" with N and Δ trajectories,[24] is also shown in the figure (dashed curve). Though our results are slightly poorer than those of Ref. 24, the agreement with the experiment is very satisfactory indeed. Thus the s-channel resonances seem to have provided an understanding of differential cross section peaks in the forward as well as backward directions (which otherwise require separate t- and u-channel calculations), and hence a rather encouraging test of the duality hypothesis.

Density Matrices

The density matrices for the same processes are shown in Figs. 6–9. The data on the density matrices are meager, the numbers are less reliable since the errors are much larger, and sometimes only the average values over a wide range of angles are available. Because of these reasons the comparison with experiment here is more or less tentative.

First of all we observe that our model predicts

$$\rho_{1\,-1} \approx 0$$

at all energies and angles. This is by and large consistent with experiment since $\rho_{1\,-1}$ is rather small compared with other elements, particularly at low energies.[13] At higher energies the discrepancy is undoubtedly large as was also the case with differential cross sections.

As for the diagonal element ρ_{00}, the agreement with experiment is very satisfactory in general. The peripheral-model predictions for the density matrix for these processes are not extensively available, so a comparison with that model cannot be performed. However, for $\pi^+p \to \rho^+p$ at 2.75 GeV/c, the peripheral-model prediction [dashed curve in Fig. 6(a)], as given in Ref. 11, is strikingly different from ours. The only available result is the value of ρ_{00} averaged over the production angle, a number which is in very good agreement with our value. A more detailed analysis of ρ_{00} will therefore be welcome.

An extensive density-matrix analysis for $\pi N \to \rho N$ has been given by Dass and Froggatt in the Regge-pole model with evasive and conspiring pion poles.[13] The results of our analysis are in qualitative agreement with those of Dass and Froggatt.

As for the $\pi^+n \to \omega p$ reaction, the data are even poorer, and only averages over rather large angles are available. Qualitatively the agreement seems to be quite good but nothing more definite can be said unless more accurate data are made available. It is interesting to observe that the simple OPE and the Regge-pole models both predicted $\rho_{00} \equiv 0$ in contrast to the experimental value which is ~0.6. In the peripheral model the situation was remedied by the inclusion of absorption effects, and in the Regge-pole model by the inclusion of B trajectory or the effect of Regge cuts, etc. At 3.25 GeV/c, where only one experimental point is known,[31] our results are in qualitative agreement as far as ρ_{00} is concerned. Relatively more data are available at 3.65 GeV/c (Ref. 32) and our results are clearly in better agreement with experiment than those of Ref. 32, using the Regge-pole model with cuts [Fig. 4(b), dashed curve], which in turn is an im-

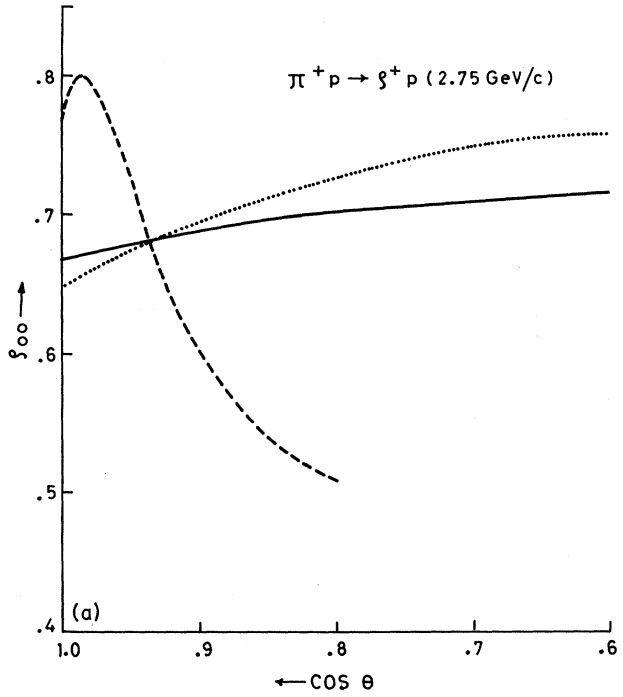

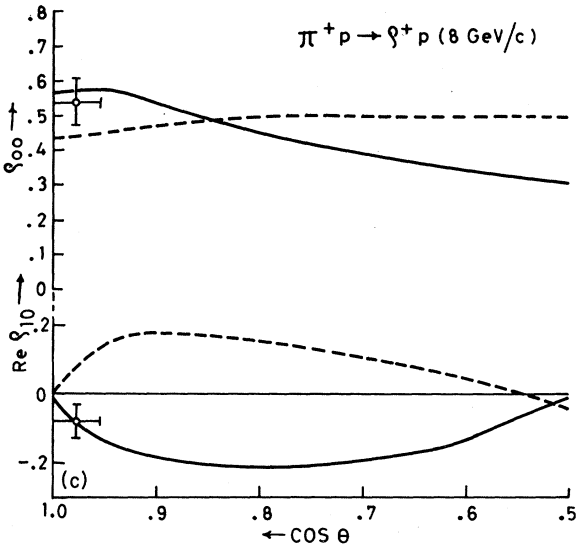

FIG. 6. (a) The density-matrix element (ρ_{00}) for the process $\pi^+ p \to \rho^+ p$ at 2.75 GeV/c. The solid and the dotted curves represent our results for new and old form factors, respectively. The dashed curve is the peripheral-model prediction by Jackson *et al.* (Ref. 11). (b) The density-matrix elements ρ_{00} and Reρ_{10} for the process $\pi^+ p \to \rho^+ p$ at 4.0 GeV/c. The experimental data are from (Ref. 13). The solid and dashed curves are our results with new and old form factors, respectively. (c) Same as at 8.0 GeV/c.

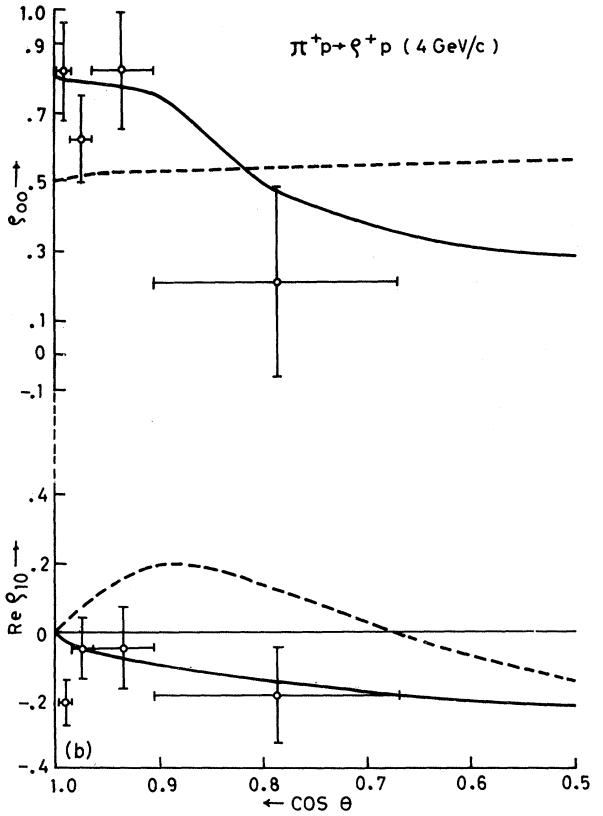

provement over an earlier calculation of Henyey *et al.*[15] Figure 6 shows our results for the density matrix for $\pi^+ p \to \rho^+ p$ with both the "old" and the "new" form factors for the purpose of comparison between the two. As in the case of differential cross section, the agreement for ρ_{00} seems to be definitely better with the "new" form factor, on the basis of the data at 4.0 GeV/c [Fig. 6(b)]. Qualitatively the difference between the results of the two form factors is the same at all the three energies plotted, though at other energies a comparison with experiment cannot be made at present because of nonavailability of data.

Whereas the difference between the predictions of the two form factors for ρ_{00} is only qualitative, the one for Reρ_{10} is striking. The "old" form factor predicts the wrong sign for Reρ_{10}, viz., positive in all cases, whereas the experimental numbers for this quantity are consistently negative for all the processes considered.[33] The "new" form factor not only reverses the sign of Reρ_{10} to bring it in agreement with the experiment, but produces

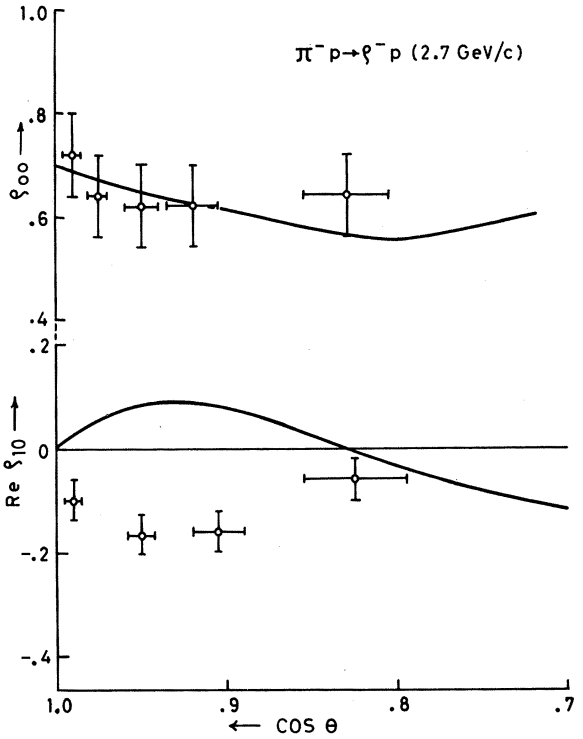

FIG. 7. The density-matrix elements ρ_{00} and $\mathrm{Re}\rho_{10}$ for the process $\pi^- p \to \rho^- p$ at 2.7 GeV/c. The curves represent our result with the new form factor. The experimental points are from Ref. 31.

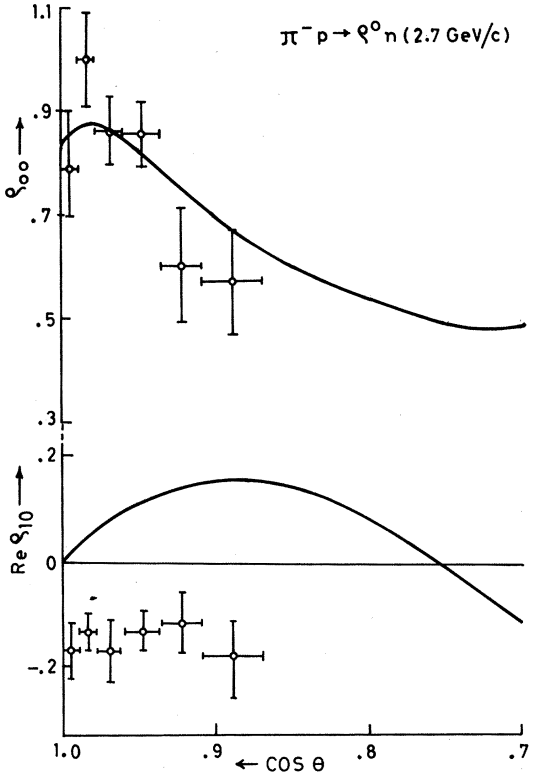

FIG. 8. Same as Fig. 7 for the process $\pi^- p \to \rho^0 n$ at 2.7 GeV/c.

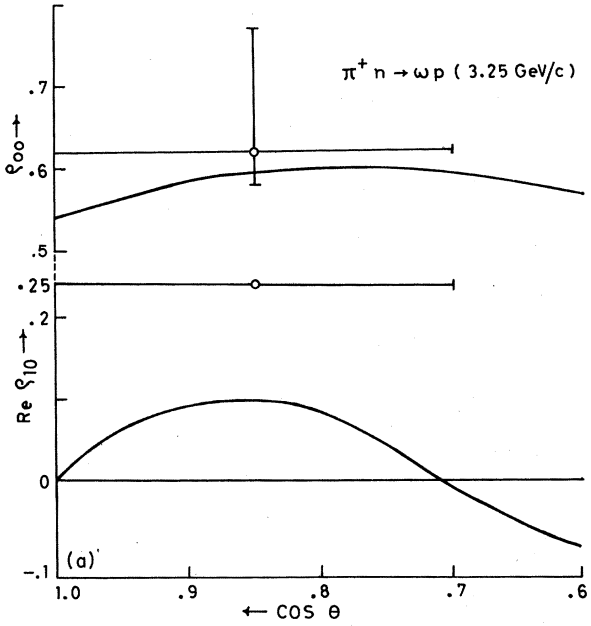

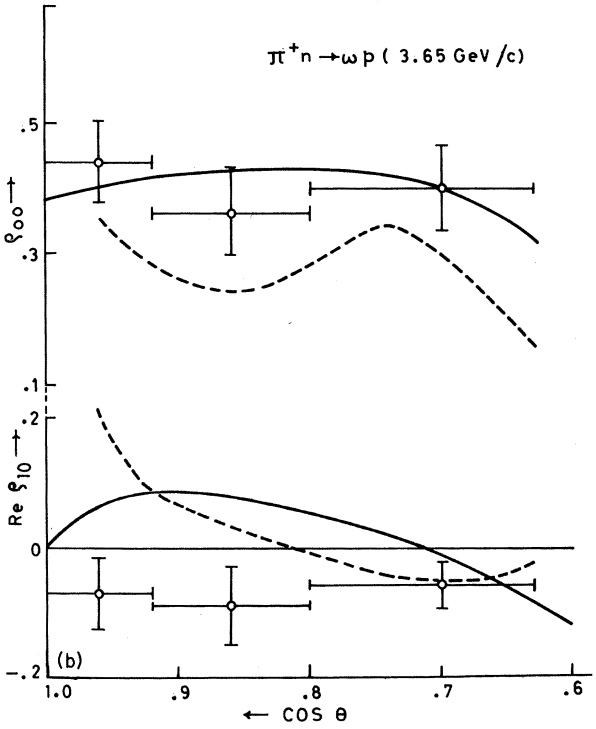

FIG. 9. (a) Same as Fig. 7 for the process $\pi^+ n \to \omega p$ at 3.25 GeV/c. The experimental point is from Ref. 31. (b) Same as in (a) at 3.65 GeV/c, compared with the experimental points from Ref. 24. The solid curve is our result with the old form factor and the dashed curve is the Regge-pole-model prediction of Ref. 32.

very good agreement even in absolute value. $\mathrm{Re}\rho_{10}$ is perhaps a quantity which depends more crucially than others on the relative phase and magnitude of various partial amplitudes, so that this agreement of $\mathrm{Re}\rho_{10}$ for the "new" form factor strongly suggests its superiority over the "old" one.

In conclusion, we find that by and large our model provides a good description of the vector-meson production processes. The agreement with experiment is from "reasonably good" to "excellent," both for the differential cross section and the density-matrix quantities which are very model dependent. As expected, the validity of the present calculation is limited to the intermediate-energy region. This range of validity can presumably be increased with the inclusion of more resonances without any extra parameters but with enormous increase in algebraic work. The results seem definitely to be in favor of the "new" form factor, as can be most clearly seen from the change even in the sign of $\mathrm{Re}\rho_{10}$ required by experiment. The calculation also provides some welcome indications of duality through a simultaneous fit to the data in the forward and the backward directions for $\pi^- p \to \rho^0 n$. Finally it may be added that more accurate data, especially a fine-grain analysis of the angular dependence of density matrices, is required for a quantitative comparison of various models available at present.

ACKNOWLEDGMENTS

We are grateful to Professor A. N. Mitra for suggesting the problem and for many illuminating discussions. It is a pleasure to acknowledge the active help and close association of Dr. D. K. Choudhury during the early stages of this investigation.

APPENDIX A

The general structure of the amplitude for the process $P+N \to V+N'$ is given by[19]

$$M_{PV}=\bar{u}(p_2)\gamma_5[C_1 i(\epsilon\cdot\gamma)+C_2(\epsilon\cdot Q)+C_3(\epsilon\cdot\gamma)(k'\cdot\gamma)+C_4 i(\epsilon\cdot Q)(k'\cdot\gamma)+C_5(\epsilon\cdot k)+C_6 i(\epsilon\cdot k)(k'\cdot\gamma)]u(p_1). \tag{A1}$$

However, we find that in our model, for the $L\pm\frac{1}{2}$ couplings mentioned as the A, B, C types in the text, the first four coefficients, namely, C_1, C_2, C_3, and C_4, exist, while the other two coefficients C_5 and C_6 receive contribution from $L+\frac{3}{2}$ (D type) coupling only.

Let

$$\begin{aligned}
&\bar{u}(p_2) i\gamma_5(\epsilon\cdot\gamma)u(p_1)=A_1,\\
&\bar{u}(p_2)\gamma_5(\epsilon\cdot Q)u(p_1)=A_2,\\
&\bar{u}(p_2)\gamma_5(\epsilon\cdot\gamma)(k'\cdot\gamma)u(p_1)=A_3,\\
&\bar{u}(p_2) i\gamma_5(\epsilon\cdot Q)(k'\cdot\gamma)u(p_1)=A_4,\\
&\bar{u}(p_2)\gamma_5(\epsilon\cdot k)u(p_1)=A_5,\\
&\bar{u}(p_2) i\gamma_5(\epsilon\cdot k)(k'\cdot\gamma)u(p_1)=A_6.
\end{aligned} \tag{A2}$$

The above invariant amplitudes are combined in the following way so that the ρ and ω production amplitudes could be conveniently expressed in terms of these combinations:

$$\begin{aligned}
a_1&=(m_\pi^2+2Q\cdot k)(mA_1-A_3)-2m(A_4-mA_3),\\
a_2&=(m_\pi^2+2Q\cdot k)A_1-2(A_4-mA_3),\\
a_3&=-(m_\pi^2+2Q\cdot k)A_1-m(2A_2+A_3),\\
a_4&=2A_2+A_3,\\
a_5&=(m_\pi^2+2Q\cdot k)A_2+(M+m)A_4,\\
a_6&=(m_\pi^2+2Q\cdot k)(S-Mm)A_2+m_\pi^2 MA_4,\\
a_7&=[m_\pi^2-(Q\cdot k/M^2)(Q^2+Mm)]A_2+(m-M-Q\cdot k/M)A_4,\\
b_1&=mA_1+2A_2+A_3,\\
b_2&=-[m_\pi^2+2(Q\cdot k)]A_1-mA_3+2A_4,\\
b_3&=-A_4+(Q\cdot k/M)A_3,\\
b_4&=(Q\cdot k)a_2+(Q\cdot k')m_\pi^2 A_1,
\end{aligned}$$

$$b_5 = A_4(m+M),$$

$$b_6 = -[(Q^2+Mm)A_2 + (Q\cdot k)A_3],$$

$$b_7 = (m_\pi{}^2 + 2Q\cdot k)A_5 + (M+m)A_6,$$

$$b_8 = (m_\pi{}^2 + 2Q\cdot k)(s-Mm)A_5 + m_\pi{}^2 MA_6,$$

$$b_9 = [m_\pi{}^2 - (Q\cdot k/M^2)(Q^2+Mm)]A_5 + (m-M-Q\cdot k/M)A_6,$$

$$I_1 = -\tfrac{1}{5}\left(F - 10\frac{(Q\cdot k)(Q\cdot k')}{M^2}\right)a_1 - \tfrac{1}{5}MFa_2 - \frac{Q\cdot k}{M}m_V{}^2 a_3 - m_V{}^2(Q\cdot k)\left(2+\frac{Q^2}{M^2}\right)a_4$$
$$- m_\pi{}^2 m_V{}^2 b_1 - m_\pi{}^2 b_2\frac{Q\cdot k}{M} - m_\pi{}^2 m_V{}^2 MA_1 + m_\pi{}^2(Q\cdot k')\frac{Q^2}{M^2}A_3,$$

$$I_2 = \tfrac{1}{5}(a_3 - Ma_4)F' + 3\left[(m_\pi{}^2 + 2Q\cdot k)\left(a_2 + \frac{Q\cdot k'}{M}a_4 + b_3\right) - m_\pi{}^2(m+M)a_4 + \frac{Q^2-Mm}{M^2}b_4\right],$$

$$I_3 = a_1 + Ma_2 - \frac{1}{M}[(Q\cdot k')a_3 + (Q\cdot k)b_2] - \frac{Q^2}{M^2}(Q\cdot k')a_4 - \tfrac{1}{5}\left(F(b_1+MA_1) - 10\frac{(Q\cdot k)(Q\cdot k')}{M^2}b_1\right),$$

$$I_4 = \frac{Q\cdot k'}{M}\left(a_1 - \frac{Q^2}{M}a_2 - \frac{2(Q\cdot k)}{M}b_2\right) - m_V{}^2\left[a_3 - Ma_4 - \frac{Q\circ k}{M}b_1 + Q\cdot k\left(2+\frac{Q^2}{M^2}\right)A_1 + \tfrac{1}{5}Fb_2\right],$$

$$I_5 = F_4\left\{(Q\cdot k)\left[\frac{a_1}{M} - \left(\tfrac{4}{5}+\frac{Q^2}{M^2}\right)a_2 + 2\frac{Q\cdot k'}{M^2}a_3\right] + m_\pi{}^2(Q\cdot k')\left(\frac{b_1}{M} - \frac{Q^2}{M^2}A_1\right) + \tfrac{2}{5}m_\pi{}^2(b_2 + MA_3)\right\} + F_7(a_3 - ma_4),$$

$$I_6 = F_4\left[m_\pi{}^2\frac{Q\cdot k'}{M^2}(Q^2A_3 - Mb_2) - m_V{}^2(Q\cdot k)\left(\tfrac{4}{5}+\frac{Q^2}{M^2}\right)a_4 - \tfrac{2}{5}m_V{}^2 m_\pi{}^2\left(b_1\frac{Q\cdot k}{M^2} + MA_1\right)\right.$$
$$\left. - 2\frac{(Q\cdot k)(Q\cdot k')}{M^2}a_4 - \frac{Q\cdot k}{M}m_V{}^2 a_3\right] - F_7(a_1 + Ma_2),$$

$$I_7 = \tfrac{1}{3}\left\{(F_5+F_6)[-(m+M)a_2 + m_\pi{}^2 A_3] - F_6 m_V{}^2(b_1 - MA_1)\right.$$
$$\left. + \left[F_5\frac{Q\cdot k}{M^2} + F_6\frac{Q\cdot k'}{M^2} + F_8\frac{Q\cdot k}{M^2}\left(2-\frac{s}{M^2}\right)\right][-Ma_2 + (a^2+Mm)A_3] - F_6 m_V{}^2(b_1 - MA_1)\right\},$$

$$I_8 = [F_{10} + 9x(\tfrac{1}{10}F_8 - 3F_4{}^2)](b_1 - MA_1)$$
$$+ 9(\tfrac{1}{10}F_8 - 3F_4{}^2)\left(a_2(m+2M) + A_3(Q^2 - Mm - m_\pi{}^2) + \frac{Q\cdot k'}{M^2}[a_4(Mm - Q^2) + A_1M(Q^2 + m^2 - 2Q\cdot k)]\right),$$

$$I_9 = -F_9 b_7 + 135F_4\left(-xb_7 + \frac{Q\cdot k'}{M^2}b_8 + m_V{}^2 b_9\right) - \left(\frac{Q\cdot k}{M^2}F_9 + \frac{Q\cdot k'}{M^2}F_{12} + F_{11}\right)a_5$$
$$+ \frac{9}{M^2}(\tfrac{1}{10}F_8 - 3F_4{}^2)\left(a_6 - \frac{Q^2}{M^2}(Q\cdot k)a_5\right) + \frac{9}{M^2}[15(Q\circ k)F_4 - 3(Q\cdot k')F_4']\left(xa_5 + \frac{Q\cdot k'}{M^2}a_6 + m_V{}^2 a_7\right)$$
$$+ 9(\tfrac{1}{10}F_8 - 3F_4{}^2)\left[-a_2\left(m+M+\frac{Q\cdot k}{M}\right) + A_3\left(m_\pi{}^2 - \frac{Q\cdot k}{M^2}Q^2 - \frac{Q\cdot k}{M}m\right) - 2\left(b_7 + a_5\frac{Q\cdot k}{M}\right)\right],$$

$$I_{10} = (b_1 - mA_1)\left(10\frac{(Q\cdot k)(Q\cdot k')}{M^2} - F\right) + 5\frac{Q\cdot k'}{M^2}(s+Mm)a_4 + 5m_\pi{}^2[A_1(m+M) - A_3]$$
$$+ \frac{5}{M}[b_4 + 2m(Q\cdot k)A_2] + 5(m+M)(a_2 - m_\pi{}^2 A_1) + 5\frac{Q^2}{M^2}(Q\cdot k)A_3,$$

$$I_{11} = \left[-5(m+M)a_2 + 5\frac{Q\cdot k}{M}(A_1 + 2A_4) - \frac{Q\cdot k}{M^2}\left(7 - \frac{2s}{M^2}\right)b_5\right.$$
$$\left. + \frac{5m_\pi{}^2}{M}(A_4 + MA_3) + \frac{5}{M^2}(m_\pi{}^2 + 2Q\cdot k)b_6 - 3\left(6 - \frac{s}{M^2}\right)b_7\right],$$

$$I_1' = (F_2 - 6F_4')\left(m_V{}^2(b_1 - A_1M) - \frac{Q\cdot k'}{M^2}b_{10}\right) + (30F_4 + F_1)[-a_2(m+M) + m_\pi{}^2 A_3]$$

$$+\frac{Q\cdot k}{M^2}\left[-F_1(Ma_2+Q^2A_3+MmA_3)+30F_4\left(2+\frac{Q^2}{M^2}\right)b_{10}\right]-6F_4'\left(1+\frac{Q^2}{M^2}\right)\frac{(Q\cdot k)(Q\cdot k')}{M^2}[a_2-(M+m)A_3],$$

$$I_2'=\left\{F_3+21F_4\left[k\cdot k'+\frac{(Q\cdot k)(Q\cdot k')}{M^2}\left(2+\frac{Q^2}{M^2}\right)\right]\right\}(a_3-Ma_4)$$

$$+21F_4\left((Q^2+m^2)a_2-A_3m_\pi^2(m+M)+\frac{Q\cdot k'}{M^2}[m_\pi^2(Q^2-Mm)A_1-M(Q^2+m^2)a_4]\right.$$

$$\left.+\frac{Q\cdot k}{M^2}[a_2(Q^2-Mm)+MA_3(Q^2+m^2)]\right),$$

$$I_3'=-F_{13}b_7+21\left(-xb_7+\frac{Q\cdot k'}{M^2}b_8\right)+m_\rho^2b_9-a_5\left(\frac{Q\cdot k}{M^2}F_{13}+\frac{Q\cdot k'}{M^2}F_{14}+F_{15}+21F_4\frac{Q^2(Q\cdot k)}{M^4}\right)$$

$$+21\frac{Q\cdot k}{M^2}\left(-xa_5+\frac{Q\cdot k'}{M^2}a_6+m_\rho^2a_7\right)+21F_4a_6+21F_4\left(-a_2(m+M)+m_\pi^2A_3-2b_7\right.$$

$$\left.+\frac{Q\cdot k}{M^2}(-Ma_2-2a_3+MmA_3-Q^2A_3)\right),$$

where x, F, F', F_i are all functions of the kinemetical variables, viz.,

$$x=2k\cdot k'+\frac{(Q\cdot k)(Q\cdot k')}{M^2}\left(2+\frac{Q^2}{M^2}\right),$$

$$F=\left(6+\frac{Q^2}{M^2}\right)\left(3k\cdot k'+4\frac{(Q\cdot k)(Q\cdot k')}{M^2}\right),$$

$$F'=F-2\frac{(Q\cdot k)(Q\cdot k')}{M^2}\left(5+2\frac{Q^2}{M^2}\right),$$

$$F_1=6\left(6+\frac{Q^2}{M^2}\right)F_4+12\frac{(Q\cdot k)(Q\cdot k')}{M^2}\left(1+\frac{Q^2}{M^2}\right),$$

$$F_2=15\left[F_4'+\left(\frac{Q\cdot k}{M}\right)^2\left(1+\frac{Q^2}{M^2}\right)\right]-30\left(4+\frac{Q^2}{M^2}\right)F_4',$$

$$F_3=\tfrac{15}{2}\left(4+\frac{Q^2}{M^2}\right)F_4^2-12F_4\left[F_4+\frac{(Q\cdot k)(Q\cdot k')}{M^2}\left(1+\frac{Q^2}{M^2}\right)\right]$$

$$-3F_4''\left[F_4'+\left(\frac{Q\cdot k}{M}\right)^2\left(1+\frac{Q^2}{M^2}\right)\right]-3F_4'\left[F_4''+\left(\frac{Q\cdot k'}{M}\right)^2\left(1+\frac{Q^2}{M^2}\right)\right]-\tfrac{3}{2}\left(4+\frac{Q^2}{M^2}\right)F_4'F_4'',$$

$$F_4=k\cdot k'+(Q\cdot k)(Q\cdot k')/M^2,$$

$$F_4'=-m_\pi^2+(Q\cdot k/M)^2,$$

$$F_4''=-m_V^2+(Q\cdot k'/M)^2,$$

$$F_5=-15F_4^2\left(8+\frac{Q^2}{M^2}\right)-60F_4\frac{(Q\cdot k)(Q\cdot k')}{M^2}\left(1+\frac{Q^2}{M^2}\right)+6\left(4+\frac{Q^2}{M^2}\right)F_4'F_4''$$

$$-15F_4''\left[F_4'+\left(\frac{Q\cdot k}{M}\right)^2\left(1+\frac{Q^2}{M^2}\right)\right]+12F_4'\left[F_4''+\left(\frac{Q\cdot k'}{M}\right)^2\left(1+\frac{Q^2}{M^2}\right)\right],$$

$$F_6=F_4\left[15m_\pi^2\left(7+3\frac{Q^2}{M^2}\right)+60\frac{Q^2}{M^2}\left(\frac{Q\cdot k}{M}\right)^2\right]-30\frac{(Q\cdot k)(Q\cdot k')}{M^2}\left(1+\frac{Q^2}{M^2}\right)F_4',$$

$$F_7=\tfrac{1}{35}\left(4+\frac{Q^2}{M^2}\right)\left(\tfrac{125}{4}F_4^2-F_4'F_4''\right)+F_4\left(-\tfrac{4}{7}(x-k\cdot k')+\frac{(Q\cdot k)(Q\cdot k')}{M^4}Q^2\right)$$

$$-\tfrac{2}{35}\left\{2m_\pi^2m_V^2-\left(3+\frac{Q^2}{M^2}\right)\left[m_\pi^2\left(\frac{Q\cdot k'}{M}\right)^2+m_V^2\left(\frac{Q\cdot k}{M}\right)^2\right]+\left(\frac{(Q\cdot k)(Q\cdot k')}{M^2}\right)^2\left(4+2\frac{Q^2}{M^2}\right)\right\},$$

$$F_8=105F_4^2-15F_4'F_4'',$$

$$F_9=\tfrac{15}{2}F_4^2\left(16+7\frac{Q^2}{M^2}\right)-60F_4\frac{(Q\cdot k)(Q\cdot k')}{M^2}\left(1+\frac{Q^2}{M^2}\right)-\tfrac{3}{2}F_4'F_4''\left(12+5\frac{Q^2}{M^2}\right)$$
$$-15F_4''\left[F_4'+\left(\frac{Q\cdot k}{M}\right)^2\left(1+\frac{Q^2}{M^2}\right)\right]-15F_4'\left[F_4''+\left(\frac{Q\cdot k'}{M}\right)^2\left(1+\frac{Q^2}{M^2}\right)\right],$$

$$F_{10}=F_4F_9-5F_4^3\left(16+7\frac{Q^2}{M^2}\right)+3\frac{(Q\cdot k)(Q\cdot k')}{M^2}\left(1+\frac{Q^2}{M^2}\right)\left(10F_4^2+4F_4'F_4''\right),$$

$$F_{11}=6\left(1+\frac{Q^2}{M^2}\right)\left(\frac{Q\cdot k}{M^2}(-5F_4^2+2F_4'F_4'')-6\frac{Q\cdot k'}{M^2}F_4F_4'\right),$$

$$F_{12}=-3F_4\left[-m_\pi^2\left(32+5\frac{Q^2}{M^2}\right)+3\left(\frac{Q\cdot k}{M}\right)^2\left(14+5\frac{Q^2}{M^2}\right)\right]+24\frac{(Q\cdot k)(Q\cdot k')}{M^2}\left(1+\frac{Q^2}{M^2}\right)F_4',$$

$$F_{13}=3k\cdot k'\left(12+5\frac{Q^2}{M^2}\right)+3\frac{(Q\cdot k)(Q\cdot k')}{M^2}\left(8+\frac{Q^2}{M^2}\right),$$

$$F_{14}=3m_\pi^2\left(8+\frac{Q^2}{M^2}\right)-3\left(\frac{Q\cdot k}{M}\right)^2\left(10+\frac{3Q^2}{M^2}\right),$$

$$F_{15}=-3\left(4+\frac{Q^2}{M^2}\right)F_4-F_6\left[F_4'+\left(\frac{Q\cdot k}{M}\right)^2\left(1+\frac{Q^2}{M^2}\right)\right]-6F_4'.$$

APPENDIX B

In this appendix we list the expressions for the invariant amplitudes $\bar{u}(p_2)O_iu(p_1)=\langle\lambda,\lambda_f|O_i|\lambda_i\rangle$ in terms of the kinematical variables of the different particles. The other amplitudes can be obtained from these through the relation

$$\langle\lambda,\lambda_f|O_i|\lambda_i\rangle=(-1)^{\lambda+\lambda_f+\lambda_i}\langle-\lambda,-\lambda_f|O_i|-\lambda_i\rangle.$$

$$\langle\pm\tfrac{1}{2},\pm1|O_i|\pm\tfrac{1}{2}\rangle=0,\quad\text{for}\quad i=1,2,3,4$$

$$\langle+\tfrac{1}{2},-1|O_1|\tfrac{1}{2}\rangle=-\frac{2}{K_1}m_1\sin\tfrac{1}{2}\theta,$$

$$\langle-\tfrac{1}{2},1|O_1|\tfrac{1}{2}\rangle=\frac{2}{K_1}m_2\cos\tfrac{1}{2}\theta,$$

$$\langle\tfrac{1}{2},0|O_1|\tfrac{1}{2}\rangle=\frac{1}{K_2}(w_{k'}m_1+|k'|n_1)\cos\tfrac{1}{2}\theta,$$

$$\langle-\tfrac{1}{2},0|O_1|\tfrac{1}{2}\rangle=\frac{1}{K_2}(-w_{k'}m_2+|k'|n_1)\sin\tfrac{1}{2}\theta,$$

$$\langle-\tfrac{1}{2},1|O_2|\tfrac{1}{2}\rangle=0,$$

$$\langle+\tfrac{1}{2},-1|O_2|+\tfrac{1}{2}\rangle=0,$$

$$\langle-\tfrac{1}{2},0|O_2|\tfrac{1}{2}\rangle=-\frac{|k'|}{K_2}w\sin\tfrac{1}{2}\theta n_1,$$

$$\langle\tfrac{1}{2},0|O_2|\tfrac{1}{2}\rangle=-\frac{|k'|}{K_2}w\cos\tfrac{1}{2}\theta n_2,$$

$$\langle-\tfrac{1}{2},1|O_3|\tfrac{1}{2}\rangle=\frac{2w_{k'}}{K_1}\left(m_1+\frac{|k'|}{w_{k'}}n_1\right)\cos\tfrac{1}{2}\theta,$$

$$\langle\tfrac{1}{2},-1|O_3|\tfrac{1}{2}\rangle=-\frac{2w_{k'}}{K_1}\sin\tfrac{1}{2}\theta\left(m_2-\frac{|k'|}{w_{k'}}n_1\right),$$

$$\langle\tfrac{1}{2},0|O_3|\tfrac{1}{2}\rangle=-2\frac{w_{k1}^2-m_V^2}{K_2}\cos\tfrac{1}{2}\theta m_2,$$

$$\langle-\tfrac{1}{2},0|O_3|\tfrac{1}{2}\rangle=2\frac{w_{k'}^2-m_V^2}{K_2}m_1\sin\tfrac{1}{2}\theta,$$

$$\langle\tfrac{1}{2},-1|O_4|\tfrac{1}{2}\rangle=0,$$

$$\langle-\tfrac{1}{2},1|O_4|\tfrac{1}{2}\rangle=0,$$

$$\langle\tfrac{1}{2},0|O_4|\tfrac{1}{2}\rangle=-\frac{2|k||k'|w}{K_2}\left(m_1+n_1\frac{k_0}{|k|}\right)\cos\tfrac{1}{2}\theta,$$

$$\langle-\tfrac{1}{2},0|O_4|\tfrac{1}{2}\rangle=-\frac{2|k||k'|w}{K_2}\left(m_1+n_1\frac{k_0}{|k|}\right)\sin\tfrac{1}{2}\theta,$$

$$\langle\tfrac{1}{2},1|O_5|\tfrac{1}{2}\rangle=-\langle\tfrac{1}{2},-1|O_5|\tfrac{1}{2}\rangle=\frac{|k|}{K_1}n_2\sin\theta\cos\tfrac{1}{2}\theta,$$

$$\langle\tfrac{1}{2},0|O_5|\tfrac{1}{2}\rangle=\frac{1}{K_2}(|k|w_{k'}\cos\theta-|k'|k_0)n_2\cos\tfrac{1}{2}\theta,$$

$$\langle-\tfrac{1}{2},0|O_5|\tfrac{1}{2}\rangle=\frac{1}{K_2}(|k|w_{k'}\cos\theta-|k'|k_0)n_1\sin\tfrac{1}{2}\theta,$$

$$\langle-\tfrac{1}{2},1|O_5|\tfrac{1}{2}\rangle=-\langle-\tfrac{1}{2},-1|O_5|\tfrac{1}{2}\rangle=\frac{|k|}{K_1}n_1\sin\theta\sin\tfrac{1}{2}\theta,$$

$$\langle\tfrac{1}{2},1|O_6|\tfrac{1}{2}\rangle=-\langle\tfrac{1}{2},-1|O_6|\tfrac{1}{2}\rangle$$
$$=\frac{|k|}{K_1}(|k'|m_1+w_{k'}n_1)\sin\theta\cos\tfrac{1}{2}\theta,$$

$$\langle\tfrac{1}{2},0|O_6|\tfrac{1}{2}\rangle=\frac{1}{K_2}(|k|w_{k'}\cos\theta-|k'|k_0)$$
$$\times(|k'|m_1+w_{k'}n_1)\cos\tfrac{1}{2}\theta,$$

$$\langle-\tfrac{1}{2},0|O_6|\tfrac{1}{2}\rangle=-\frac{1}{K_2}(|k|w_k'\cos\theta-|k'|k_0)$$
$$\times(m_2\times|k'|-w_k'n_2)\sin\tfrac{1}{2}\theta,$$

$$\langle -\tfrac{1}{2}, 1 | O_6 | \tfrac{1}{2} \rangle = -\langle -\tfrac{1}{2}, -1 | O_6 | \tfrac{1}{2} \rangle$$
$$= -\frac{|k|}{K_1}(|k'|m_2 - w_k' n_2)\sin\theta \sin\tfrac{1}{2}\theta,$$

where

$$K_1 = 2m[2(E_1+m)(E_2+m)]^{1/2},$$
$$K_2 = 2mm_\rho[(E_1+m)(E_2+m)]^{1/2},$$
$$m_{1,2} = (E_1+m)(E_2+m) \pm |p_1||p_2|,$$
$$n_{1,2} = (E_1+m)(E_2+m)\left(\frac{|p_1|}{E_1+m} \pm \frac{|p_1|}{E_2+m}\right),$$
$$w = \sqrt{S}.$$

E_1 (E_2) and k_0 ($w_{k'}$) are, respectively, the energies of the incident (final) nucleon and pion (vector meson).

---

[1]Rashmi Mehrotra and A. N. Mitra, preceding paper, Phys. Rev. D 5, 1803 (1972).

[2]A. N. Mitra, in *Lectures in High Energy Theoretical Physics*, edited by H. H. Aly (Gordon and Breach, London, 1970).

[3]A. N. Mitra, Nuovo Cimento 61A, 344 (1969).

[4]A. N. Mitra, Nuovo Cimento 64A, 603 (1969).

[5]S. Das Gupta and B. K. Mohana, Nuovo Cimento 64A, 325 (1969).

[6]D. L. Katyal and A. N. Mitra, Phys. Rev. D 1, 338 (1970).

[7]D. K. Choudhury and A. N. Mitra, Phys. Rev. D 1, 351 (1970).

[8]J. D. Jackson and H. Pilkuhn, Nuovo Cimento 33, 906 (1964); 34, 1841 (1964).

[9]K. Gottfried and J. D. Jackson, Nuovo Cimento 34, 735 (1964); 34, 1843 (1964).

[10]M. H. Ross and G. L. Shaw, Phys. Rev. Letters 12, 627 (1964).

[11]J. D. Jackson, J. T. Donohue, K. Gottfried, R. Keyser, and B. E. Y. Svensson, Phys. Rev. 139, B428 (1965).

[12]J. D. Jackson, Rev. Mod. Phys. 37, 484 (1965).

[13]G. V. Dass and C. D. Froggatt, Nucl. Phys. B8, 661 (1968).

[14]M. Barmawi, Phys. Rev. 142, 1088 (1965); Phys. Rev. Letters 16, 595 (1966); Phys. Rev. 166, 1857 (1968).

[15]F. Henyey, K. Kajantie, and G. L. Kane, Phys. Rev. Letters 21, 1782 (1968).

[16]R. Dolen, D. Horn, and C. Schmid, Phys. Rev. 166, 1768 (1968).

[17]G. F. Chew and A. Pignotti, Phys. Rev. Letters 20, 1078 (1968).

[18]A. N. Mitra, Ann. Phys. (N.Y.) (to be published).

[19]Lu Sun Liu and P. Singer, Phys. Rev. 135, B1017 (1964).

[20]As mentioned in Sec. I, we have considered the s-channel intermediate states with orbital angular momentum $L = 0, 1, 2$. These resonances are all listed in Table I of Ref. 1. The state $N(1470)$ of $J = \frac{1}{2}$ (Roper resonance), believed to be a radial excitation of the familiar nucleon, has also been included in the calculation.

[21]The baryon resonances B_L are assumed to have a complex mass $M_J = M - i\frac{1}{2}\Gamma_J$. The real part of the mass M and the total decay width Γ_J are taken from experiment.

[22]C. Fronsdal, Suppl. Nuovo Cimento 9, 416 (1958).

[23]R. Blankenbecler and R. L. Sugar, Phys. Rev. 168, 1597 (1968).

[24]S. Hagopian, V. Hagopian, E. Bogart, R. O'Donnell, and W. Selove, Phys. Rev. Letters 24, 1445 (1970).

[25]S. Das Gupta, V. K. Gupta, and A. N. Mitra, Phys. Rev. 172, 1482 (1968).

[26]H. J. Lipkin, F. Scheck, and H. Stern, Phys. Rev. 152, 1375 (1966).

[27]J. L. Friar and J. S. Trefil, Nuovo Cimento 49A, 642 (1967).

[28]K. Kajantie and J. S. Trefil, Nucl. Phys. B2, 243 (1967).

[29]D. H. Miller, L. Gutay, P. B. Johnson, F. J. Loeffler, R. L. McIlwain, R. J. Sprafka, and R. B. Willmann, Phys. Rev. 153, 1423 (1967).

[30]Aachen-Berlin-CERN Collaboration, Nucl. Phys. B8, 45 (1968).

[31]H. O. Cohn, W. M. Bugg, and G. T. Condo, Phys. Letters 15, 344 (1965).

[32]K. Kajantie and P. V. Ruuskanen, Nucl. Phys. B13, 437 (1969).

[33]For the process $\pi^+ n \to \omega p$, the sign of $\mathrm{Re}\,\rho_{10}$, as predicted by the "old" form factor, is positive again, but the experimental situation is not very clear. One group has reported a positive (Ref. 31) value and another negative (Ref. 15). The results of other analyses also seem to yield a positive value for this quantity. Thus nothing definite can be said about this reaction until the experimental situation crystallizes.